Applied Surface Science 306 (2014) 52–55

Contents lists available at ScienceDirect

Applied Surface Science

journal homepage: www.elsevier.com/locate/apsusc

Optical properties of amorphous indium zinc oxide thin films synthesized by pulsed laser deposition

V. Craciun[a], C. Martin[b], G. Socol[a], D. Tanner[c], H.C. Swart[d], N. Becherescu[e], D. Craciun[a,*]

[a] Lasers Department, National Institute for Lasers, Plasma and Radiation Physics, Magurele, Bucharest, Romania
[b] Ramapo College of New Jersey, NJ, USA
[c] Physics Department, University of Florida, Gainesville, FL, USA
[d] Department of Physics, University of Free State, Bloemfontein 9300, South Africa
[e] Apel Laser, 20A, Constructorilor Blvd., 060512 Bucharest, Romania

ARTICLE INFO

Article history:
Received 24 November 2013
Received in revised form 19 March 2014
Accepted 30 March 2014
Available online 12 April 2014

Keywords:
Pulsed laser deposition
Amorphous transparent and conductive oxides
Infrared reflectance
Indium zinc oxide

ABSTRACT

The optical properties of amorphous indium zinc oxide (a-IZO) films that were grown at room temperature by the pulsed laser deposition technique with the aid of a KrF excimer laser were investigated. Two values of 0.65 and 0.90 for the In/(In + Zn) films composition were chosen since they roughly define the area in the In–Zn–O phase diagram where good transmission in the visible range together with excellent electrical properties for a-IZO films were measured. The results of the investigations indicated that the IZO films containing 90 at.% In possessed excellent qualities: high transparency from 0.400 to 4 μm, high reflectivity in the mid IR range together with a very low resistivity of 5×10^{-4} Ω cm and a high mobility of 40 cm^2/V s.

1. Introduction

Flexible and transparent electronics, organics based solar cells and sensors require transparent and conductive materials that could be deposited at room temperature. One of the best materials that exhibits good transparency in the visible range, low resistivity, and high mobility has been shown to be indium zinc oxide (IZO) [1,2]. When deposited at temperatures below 100 °C, IZO is amorphous, having additional benefits such as uniformity and homogeneity [3,4].

We recently reported the synthesis of high quality amorphous IZO (a-IZO) thin films on glass substrates by the pulsed laser deposition technique (PLD) using a KrF excimer laser [5]. The PLD technique is very suitable for growing films in order to investigate the interdependence between composition, structure and properties. Depending on their particular In/(In + Zn) ratio, the films exhibited very good optical and electrical properties. We further investigated the influence of target-substrate separation distance on the quality of IZO thin films grown on polyethylene terephthalate (PET) substrates [6]. In addition to excellent electrical and optical characteristics we found that the films that were grown at the optimum target-substrate distance were homogenous, smooth, adherent, and without cracks or any other extended defects, being suitable for the study of various optoelectronic device applications.

The optical properties in the visible range of a-IZO and amorphous indium gallium zinc oxide (a-IGZO) thin films with various In/(In + Zn) and In/(In + Ga + Zn) ratios obtained by PLD were also investigated [7,8]. Starting from targets with various atomic In concentrations from 0% (pure ZnO) up to 90% In/(In + Zn) and 2% Ga/(Ga + Zn), films were grown on Si and quartz substrates. It was found that the dependence of the refractive index on composition in the transparency range was similar to the dependence of density on stoichiometry. Films with a higher indium content exhibited a more pronounced free carrier light absorption [7].

For many practical applications, the near infrared (NIR) and mid infrared (MIR) optical properties of these transparent and conductive oxide films are particularly important [9,10]. For example, indium tin oxide (ITO) and doped ZnO films, due to their metallic behavior and low losses in the NIR region, were studied as potential candidates for plasmonic applications [11–13]. Our current work is motivated by the lack of infrared optical data on a-IZO films. Therefore, we present here such measurements of optical reflectance and extracted optical conductivity on a-IZO films, for two different values of the In/(In + Zn) ratio: 0.65 and 0.90, respectively. These values

* Corresponding author. Tel.: +40 21 457 4491; fax: +40 21 457 4491.
E-mail address: doina.craciun@inflpr.ro (D. Craciun).

http://dx.doi.org/10.1016/j.apsusc.2014.03.189
0169-4332/

Table 1
Elemental composition and thickness of IZO_65 and IZO_90 thin films.

Sample	In/(In + Zn)				Thickness	
	EDAX	LIBS	RBS	XRF	RBS ($\times 10^{15}$ at/cm^2)	SE (nm)
IZO_65	0.66	0.65	0.64	0.65	4250	625
IZO_90	0.86	0.88	0.93	0.91	4100	575

roughly correspond to the limits of the compositional region in which high transparency, low resistivity and high mobility properties were previously reported [5,14,15].

2. Experimental

A KrF* laser source (model COMPexPro 205, Lambda Physics-Coherent, $\lambda = 248$ nm and $\tau_{las} = 25$ ns) was used to deposit films from IZO targets with In/(In + Zn) ratio concentrations of 65 and 90 at.% under 1 Pa oxygen atmosphere. The laser fluence onto the targets surface was around 2 J/cm^2, at a repetition rate of 10 Hz. Since we were interested in obtaining amorphous films, the quartz and Si substrates used, were kept at room temperature (RT) during the deposition process. A detailed description of the experimental set-up is given in Ref. [16].

After deposition the mass density of the films was inferred from simulations of the X-ray reflectivity curves, acquired in a parallel beam geometry with the aid of an X'Pert PRO MRD instrument, while the structure was investigated by grazing and symmetrical X-ray diffraction with the same instrument.

Since the optical and electrical properties, as well as the cost of these films depend on the In/(In + Zn) values, the chemical composition of the films was verified using several elemental analysis processes: laser-induced breakdown spectroscopy (LIBS), energy dispersive X-ray spectroscopy (EDAX), spectroscopic ellipsometry (SE), X-ray fluorescence (XRF, Horiba XGT 7000) and Rutherford backscattering spectrometry (RBS). Details about the advantages and limitations of these techniques applied to IZO elemental analysis are described elsewhere [17,18].

The thickness profile of the deposited films was obtained from optical analyses of spectroscopic ellipsometry data measured by a Woollam vertical-variable angle ellipsometer (V-VASE) [7]. The ellipsometer was equipped with a HS-190 monochromator which enables the spectral inspection of thin films.

Room temperature optical reflectance was measured from 30 cm^{-1} (4 meV) to 30,000 cm^{-1} (4 eV), using a Bruker-113v FTIR spectrometer and a Carl Zeiss microscope photometer. Given that our samples were thin films on top of a Si substrate, at least in certain spectral ranges, the measured reflectance includes also possible contribution from the substrate. In order to extract only the reflectance of the film, separate measurements of a Si substrate piece was also performed.

3. Results and discussion

The composition of the deposited films is displayed in Table 1. It should be mentioned that the LIBS, RBS, XRF and EDAX measurements were performed on several locations and the films were found to be compositionally homogeneous. The average film thickness, determined by modeling the SE and RBS data is also displayed in Table 1.

XRR curves recorded from the deposited films are displayed in Fig. 1. One can note that the critical angles for the IZO_65 and IZO_90 samples are different, since the In concentration was different. According to simulations of the recorded XRR curves, these critical angle values correspond to mass densities of 6.50 g/cm^3 and 6.75 g/cm^3, respectively. The surface roughness, also estimated from the XRR simulations, indicated that the films were smooth, with rms values of around 1 nm, similar to other reports [19,20]. The XRD pattern acquired in grazing incidence geometry from the IZO_90 film is displayed in Fig. 2. The film was not completely amorphous, besides the broad peaks located at around $2\theta = 17^\circ$ and 54°, which are indicative of an amorphous phase, there is a narrower peak located at around $2\theta = 32.5^\circ$. The asymmetric shape of this peak also indicates that it is very likely a convolution of two peaks, located at 31° and 34°, respectively. These positions are very close to the positions of the strongest diffraction lines for In_2O_3 (line (222) at 30.5799°, PDF card #00-006-0416) and ZnO (line (002) at 34.4211°, PDF card #00-036-1451). As previously discussed, in amorphous IZO some In-O octahedral and Zn-O tetrahedral arrangements were present and ordered on a very short length scale [21]. A crystallite size of around 1.9 nm was estimated from the widths of the broad peaks located at 31° and 34° using the Scherrer equation. The radius of curvature of the Si substrates after deposition, estimated from omega shifts of the substrate Si (0 0 4) peak measured in several locations across the surface, was essentially identical with that measured for the bare substrates, indicating a no or very low stress levels, as also found for IZO films deposited by other techniques [19,20].

The refractive index values measured in several points were almost constant for each sample. The refractive index at 630 nm of IZO_65 is approximately 2.00 while the one of IZO_90 is approximately 1.94, values in line with those observed in Fig. 3, which shows the measured reflectance $R(\omega)$ for the IZO_90 and IZO_65 films. At low energy, which is dominated by free carriers response, we can see that both samples have relatively high reflectance, even as high as 90% for the IZO_90 sample, characteristic to metallic behavior. Furthermore, a sharp plasma edge, associated with the plasma frequency of the free carriers can be observed in both samples above 1000 cm^{-1}. Beyond the plasma edge, fringes due to the interference between the beams reflected from the front and from the back of the film are clearly visible. This suggests that the measured data contain not only the reflectance of the thin film, but also contribution from the film-substrate interface.

The properties of the thin films were extracted using the following procedure. We fit the data assuming two layers (film and infinitely thick substrate) and considering a Lorentz-Drude (LD) model for both the film and the substrate. From the measured reflectance of the Si substrate alone, we obtain the LD parameters for the substrate. These are then fixed and only the parameters of

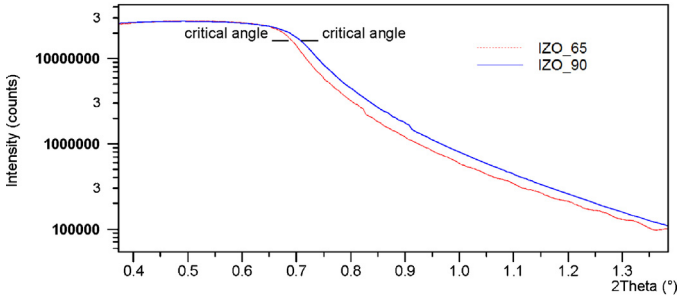

Fig. 1. XRR curves acquired from the deposited a-IZO films. The positions of the critical angle for each film are indicated by horizontal lines.

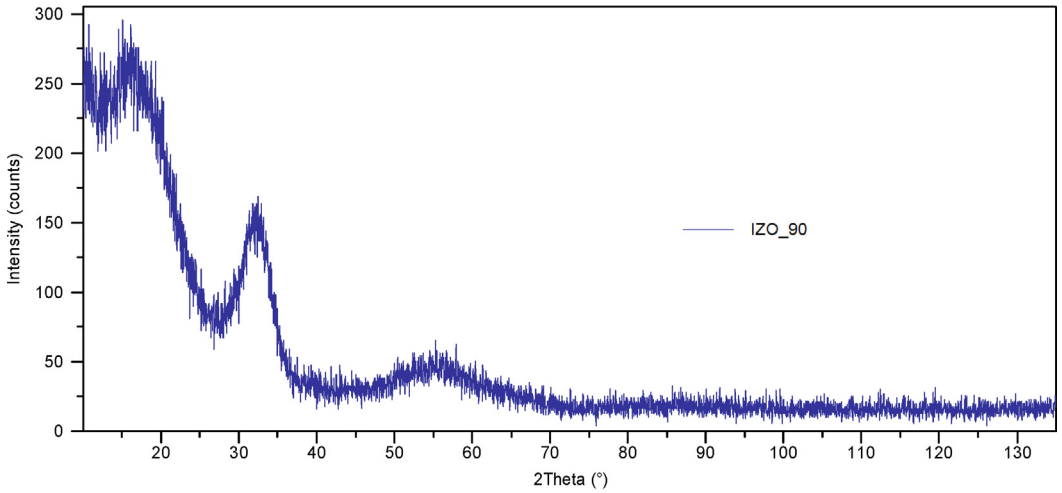

Fig. 2. XRD pattern acquired from the IZO_90 film.

the thin film are adjusted so that to reproduced the measured data. Furthermore, using the LD parameters of the film, we calculate its optical properties.

Fig. 4 shows an example (for the IZO_90 sample) of the calculated real part of optical conductivity ($\sigma_1(\omega)$). The highest frequency Lorentzian most likely corresponds to an interband transition, while the other two at lower frequencies may be associated with impurity bands, as observed in many semiconductors [22]. The free carrier (Drude) contribution is clearly visible in the limit of $\omega = 0$. Furthermore, the real part of the dielectric function ε_1, shown in the inset of Fig. 4, is negative at frequencies below a crossing point associated with the plasma frequency of the free carriers, supporting the metallic character of the samples. For the Drude plasma frequency $\omega_P = (n_0 e^2/m^* \cdot \varepsilon_0)^{1/2}$, we obtained $\omega_P \sim 11{,}000\ \mathrm{cm}^{-1}$ ($2 \times 10^{15}\ \mathrm{s}^{-1}$) for the IZO_90 film and $\omega_P \sim 5000\ \mathrm{cm}^{-1}$ ($9.5 \times 10^{14}\ \mathrm{s}^{-1}$) for the IZO_65 film, respectively. Considering the effective mass $m^* = 0.3\ m_0$ from previous theoretical studies [20,23], we obtained the free carrier concentrations $n_0 = 3.7 \times 10^{20}\ \mathrm{cm}^{-3}$ for the IZO_90 and $n_0 = 0.8 \times 10^{20}\ \mathrm{cm}^{-3}$ for the IZO_65, respectively. We also verified the electron concentration for the IZO_90 film by measuring the Hall coefficient using a four point probe in a van der Paw geometry and found an almost identical value to that reported above, underlining the validity of our optical data. The carrier concentration for the IZO_90 sample is larger than the highest values reported previously on analogous transparent conductive oxides, making IZO a promising candidate in this category [9,10].

From the LD parameters, we also obtained the scattering rates of the carriers, $1/\tau = 900\ \mathrm{cm}^{-1}$ ($1.7 \times 10^{14}\ \mathrm{s}^{-1}$) for IZO_90 and $1/\tau = 1000\ \mathrm{cm}^{-1}$ ($1.9 \times 10^{14}\ \mathrm{s}^{-1}$) for IZO_65. It can be noticed that both samples have very similar quality in terms of the scattering rate, the main difference being the electron concentration. Therefore, the mobilities $\mu = e\tau/m^*$ are very similar in both samples $\mu \sim 33$ and $\sim 40\ \mathrm{cm}^2/\mathrm{V\,s}$, respectively. These values are also larger, almost by a factor of two, than those of previous reports. We calculated the resistivity to be $\rho \sim 400\ \mu\Omega\,\mathrm{cm}$ for IZO_90 and

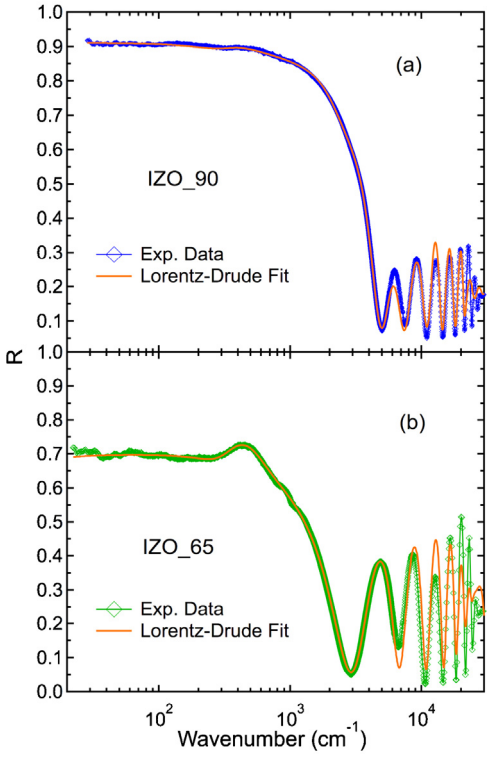

Fig. 3. Optical reflectance $R(\omega)$ of the IZO_90 (a) and IZO_65 (b) films, respectively. Symbols represent experimental data and continuous lines are fits, as explained in the main text.

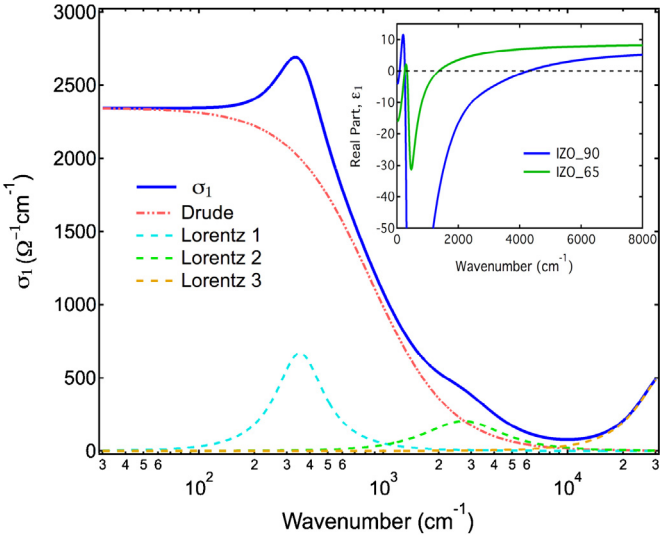

Fig. 4. Optical conductivity of the IZO_90 thin film and the Lorentz and Drude contributions. Inset shows the real part of the dielectric function for both films.

$\rho \sim 2000\ \mu\Omega$ cm for IZO_65, respectively, very similar to previously reported data [5,6].

The refractive index obtained from reflectance measurements in the visible region is $n = 2.5 \pm 0.1$, larger than the value of $n = 2$ resulted from the elipsometry data. There are possible sources of error in the estimate of n from reflectance data, like differences between the reflectance of the measured Si slab and that of the one use as a substrate, the fact that the measurements were performed on a large area, being affected by the variation of film thickness and even possible large variation of the refractive index with the wavelength. Further studies are in work to elucidate this discrepancy.

4. Conclusions

The optical properties from visible to mid IR region of amorphous IZO films deposited by the pulsed laser deposition technique at room temperature using a KrF laser were investigated. IZO films containing 90 at.% In were very transparent in the visible and near IR regions and highly reflective in the mid IR region, where they behave like metals. The films were also dense, with a smooth surface, low resistivity, high carrier concentration and high mobility.

Acknowledgments

GS, DC and VC acknowledge the financial support of PN-II-ID-PCE-2012-4-0467 project. We thank Dr. A. C. Galca for help with VASE characterization and Drs D. Pantelica and P. Ionescu for help with RBS characterization.

References

[1] J.H. Lee, B.O. Park, Thin Solid Films 426 (2003) 94–99.
[2] N.L. Dehuff, E.S. Kettenring, D. Hong, H.Q. Chiang, J.F. Wager, R.L. Hoffman, C.H. Park, D.A. Keszler, J. Appl. Phys. 97 (2005) 064505.
[3] J.C. Park, H.N. Lee, S. Im, ACS Appl. Mater. Interfaces 5 (2013) 6990–6995.
[4] A.A. Khosroabadi, P. Gangopadhyay, B. Duong, J. Thomas, A.K. Sigdel, J.J. Berry, T. Gennett, N. Peyghambarian, R.A. Norwood, Phys. Stat. Sol. A – Appl. Mater. Sci. 210 (2013) 831–838.
[5] G. Socol, D. Craciun, I.N. Mihailescu, N. Stefan, C. Besleaga, L. Ion, S. Antohe, K.W. Kim, D. Norton, S.J. Pearton, A.C. Galca, V. Craciun, Thin Solid Films 520 (2011) 1274–1277.
[6] G. Socol, M. Socol, N. Stefan, E. Axente, G. Popescu-Pelin, D. Craciun, L. Duta, C.N. Mihailescu, I.N. Mihailescu, A. Stanculescu, D. Visan, V. Sava, A.C. Galca, C.R. Luculescu, V. Craciun, Appl. Surf. Sci. 260 (2012) 42–46.
[7] A.C. Galca, G. Socol, V. Craciun, Thin Solid Films 520 (2012) 4722–4725.
[8] A.C. Galca, G. Socol, L.M. Trinca, V. Craciun, Appl. Surf. Sci. 281 (2013) 96–99.
[9] W.E. Lai, Y.H. Zhu, H.W. Zhang, Q.Y. Wen, Opt. Mater. 35 (2013) 1218–1221.
[10] T. Dhakal, A.S. Nandur, R. Christian, P. Vasekar, S. Desu, C. Westgate, D.I. Koukis, D.J. Arenas, D.B. Tanner, Sol. Energy 86 (2012) 1306–1312.
[11] G.V. Naik, V.M. Shalaev, A. Boltasseva, Adv. Mater. 25 (2013) 3264–3294.
[12] P.R. West, S. Ishii, G.V. Naik, N.K. Emani, M.V. Shalaev, A. Boltasseva, Laser Photon. Rev. 4 (6) (2010) 795–808, http://dx.doi.org/10.1002/lpor.200900055.
[13] P. Prunici, F.U. Hamelmann, W. Beyer, H. Kurz, H. Stiebig, J. Appl. Phys. 113 (2013) 123104.
[14] J.J. Lee, J.S. Kim, S.J. Yoon, Y.S. Cho, J.W. Choi, J. Nanosci. Nanotechnol. 13 (2013) 3317–3320.
[15] M.P. Taylor, D.W. Readey, C.W. Teplin, M.F.A.M. van Hest, J.L. Alleman, M.S. Dabney, L.M. Gedvilas, B.M. Keyes, B. To, J.D. Perkins, D.S. Ginley, Meas. Sci. Technol. 16 (2005) 90–94.
[16] D. Craciun, G. Socol, N. Stefan, M. Miroiu, I.N. Mihailescu, A.C. Galca, V. Craciun, Appl. Surf. Sci. 255 (2009) 5288–5291.
[17] E. Axente, J. Hermann, G. Socol, L. Mercadier, S.A. Beldjilali, M. Cirisan, C. Luculescu, C. Ristoscu, I. Mihailescu, V. Craciun, J. Anal. At. Spectrom. 29 (2014) 553–564.
[18] E. Axente, J. Hermann, G. Socol, A.C. Galca, L.M. Trinca, L. Mercadier, S.A. Beldjilali, C.R. Luculescu, D. Pantelica, P. Serban, V. Craciun, Appl. Phys. A Mater. Sci. Process. (2013), http://dx.doi.org/10.1007/s00339-014-8427-y.
[19] T. Sasabayashi, N. Ito, M. Kon, P.K. Song, K. Ustumi, A. Kajio, Y. Shigesato, Thin Solid Films 445 (2003) 219–223.
[20] N. Ito, Y. Sato, P.K. Song, A. Kaijio, K. Inoue, Y. Shigesato, Thin Solid Films 496 (2006) 99–103.
[21] A. Walsh, J.L.F. Da Silva, S.-H. Wei, J. Phys.: Condens. Matter 23 (2011) 334210.
[22] G.A. Thomas, M. Capizzi, F. DeRosa, R.N. Bhatt, T.M. Rice, Phys. Rev. B 23 (1981) 5472–5494.
[23] A. Dixit, C. Sudakar, R. Naik, V.M. Naik, G. Lawes, Appl. Phys. Lett. 95 (2009) 192105.